Indian Journal of Pure & Applied Physics
Vol. 62, March 2024, pp. 196-211
DOI: 10.56042/ijpap.v62i3.6905

Harnessing Electro-optic Effect in Directional Coupler for Implementation of Optical Digital Data Transmission Circuits

Ajay Yadav*, Ajay Kumar & Amit Prakash
Fiber Optics Laboratory, Department of Electronics and Communication Engineering,
National Institute of Technology Jamshedpur, Jharkhand 831 014, India

Received 23 November 2023; accepted 1 January 2024

The paper describes the design and implementation of optical data transmission circuits using an innovative approach based on the electro-optic effect in a directional coupler (EODC). Optical multiplexers (MUX), demultiplexers (DEMUX), encoders, decoders, and priority encoders are all included in the proposed circuit design to enable efficient and reliable data transfer. Electro-optic effect in a directional coupler have been analysed theoretically and numerically, including the detailed mathematics of coupled wave theory. The proposed device is made of $GaAlAs$ material produced from a $3\mu m \times 3\mu m$ modulator. The appropriate vale of coupling length(L_C), light wavelength, refractive index change(Δn), electric field magnitude and other parameters are considered for an efficient generation of fundamental logic gates. The design process and the simulation results provide in-depth analysis, highlighting the feasibility and utility of our approach in enhancing the performance of optical data transmission devices.

Keywords: Electro-optic effect; Directional coupler; MUX; DEMUX; Encoder; Decoder; Priority encoder

1 Introduction

The integration of optical and digital technologies has led to significant advancements in data transmission systems[1], with the electro-optic effect-based directional coupler circuit, promising enhanced efficiency and reliability. Pioneering work, as evidenced[2,3], has demonstrated the implementation of the McCulloch-Pitts neuron within directional couplers, highlighting the possibilities of harnessing this technology for sophisticated data processing. The foundational principles of quantum electronics[4] and the accompanying introduction to optical electronics[5], give crucial insights into the fundamental concepts, driving optical and digital component integration.

Moreover, the significant coupling effects inside three-arm $Ti{:}LiNbO_3$ directional couplers[6], have provided vital insight into improving coupling efficiency and thereby contributing to the evolution of data transmission capacities. Further, comprehensive works such as Integrated Optics: Theory and Technology[7] and Waves and Fields in Optoelectronics[8] have helped to build theoretical groundwork for the integration of optical and digital systems. The realization of logical gates through optical tunneling[3], along with recent advances in the implementation of Feynman Reversible and NOR logic gates via plasmonic waveguide[9], and the use of 2D photonic crystal structures for implementing optical logic gates[10], highlight the rapid progress being made in the practical application of optical digital data transmission technology. These significant advancements, together with recent studies focusing on the implementation of all-optical multiplexers[11], all-optical directional couplers for switching applications[12], and on-chip two-mode division multiplexing using directional couplers[13], collectively highlight the increasing interest and ongoing research in this domain has opened up new avenues for the development of complex optical computing systems.

Furthermore, the evaluation of performance of hybrid electro-optic directional couplers and Mach–Zehnder switches[14], as well as the investigation of engineer able switching mechanism in electro-optic directional couplers within a periodic optical superlattice[15], have demonstrated the evolving nature of this technology and its potential for customization and optimization in variety of applications. The work explores the design and implementation of optical digital data transmission combinational circuits using electro-optic effect-based directional coupler circuits, providing insights into efficient and reliable data transmission systems. Researchers have employed

*Corresponding author: (E-mail: 2021rsec010@nitjsr.ac.in)

optical approaches to enhance the performance of devices and integrated circuits, utilizing fundamental building blocks such as AND, OR, NOT, XOR, and XNOR logic gates[16,17]. Additionally, other devices, including electro-optic effect and semiconductor-optical-amplifier Mach–Zehnder Interferometer (MZI), Micro-Ring Resonator (MRR), Surface Plasmon Resonance (SPR), Fiber Bragg Grating (FBG), Photonic crystal waveguides (PCW), and Directional Coupler, have been utilized to design all-optical logic gates and switches[18–25]. The convergence of these techniques has paved the way for the development of sophisticated optical digital data transmission combinational circuits that can cater to the evolving requirements of contemporary communication system. The research on optical data transmission circuits utilizing the EODC has undergone significant evolution. The advantages of effective index-based matrix methods have been highlighted in previous studies[26], and advancements in photonic crystal technology have resulted in the development of compact terahertz DEMUX[27]. Additionally, the exploration of bi-directional couplers for mode-division has been introduced[28], along with the introduction of a compact silicon-based mode-division DEMUX[29]. Recent research has also focused on a broadband-wavelength demultiplexer utilizing sub wavelength grating-based directional couplers[30].

Our research aims to enhance EODC applicability and design optical digital data transmission combinational circuits, which will have a significant impact on future generation high-speed communication and optical communication technology development. Section 1 includes the basic introduction of optical switching activity and relevant methodology proposed by the researchers. In Section 2, the article discusses the fundamental concept of the electro-optic effect and provides a detailed mathematical description of the coupled mode theory associated with the EODC. The following sections, 3 to 7, describe the implementation of various optical circuits, including 2:1 MUX, 4:1 DEMUX, 4:2 encoder, 2:4 decoder, and priority encoder circuits and simulation results, using EODC. The discussion and conclusion of the research work are given in section 8.

The primary scientific contributions of this work lie in the design and implementation of optical data transmission circuits, employing an innovative approach using EODC. The proposed circuit integrates optical MUX, DEMUX, encoders, decoders, and priority encoders to facilitate efficient and reliable data transfer. The electro-optic effect in the directional coupler is comprehensively analyzed, both theoretically and numerically, incorporating detailed mathematics of coupled wave theory. The study considers optimal values for relevant parameters to efficiently generate fundamental logic gates. The design process and 3D simulation results for pulse propagation inside the core of the directional coupler provide visual representation, offering an in-depth analysis that underscores the feasibility and utility of our approach in enhancing the performance of optical data transmission devices.

2 Switching mechanism of Directional Coupler

A directional coupler is a significant optical device that may perform a variety of functions such as switching, sensing, and routing, modulator, power divider, etc. An electro-optic effect-based directional coupler is a device that uses the optical tunnelling phenomena to transfer electromagnetic energy from one waveguide to another. This form of coupler employs the electro-optic effect, which refers to the modification of refractive index of material in response to an applied electric field. It enables light to be transmitted from one waveguide to another, making it suitable for a variety of applications. The directional coupler is typically associated with two input and two output ports, as shown in Fig. 1. The directional coupler is a viable alternative for optical switching as it operates on the fundamental concept of electro-optic effect[2].

The change of the refractive index by an application of an electric field is the fundamental mechanism responsible for the operation of most electro-optic modulators and switches. This impact is non-isotropic in nature because it includes both linear (Pockels effect) and nonlinear (Kerr effect) components. When considering crystalline materials, the change in

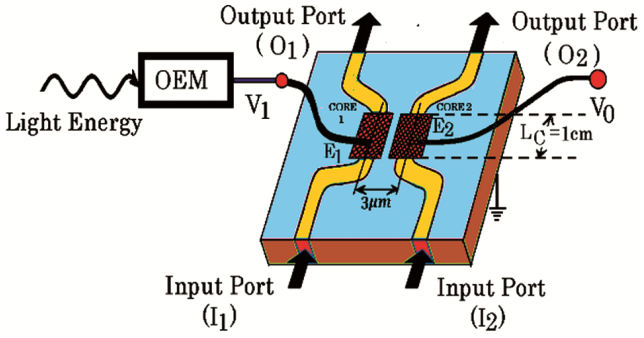

Fig. 1 — Electro-optic effect based optical directional coupler as an Optical Switch

refractive index caused by the linear electro-optic effect may be readily expressed by changes in the optical indicatrix matrix components[4]. The following equation represents the index ellipsoid in the presence of an electric field:

$$\left(\frac{1}{n^2}\right)_1 x^2 + \left(\frac{1}{n^2}\right)_2 y^2 + \left(\frac{1}{n^2}\right)_3 z^2 + 2\left(\frac{1}{n^2}\right)_4 yz + 2\left(\frac{1}{n^2}\right)_5 xz + 2\left(\frac{1}{n^2}\right)_6 xy = 1 \quad \ldots (1)$$

Here, x, y, and z align with the crystal's primary dielectric axes. The linear changes in coefficients generated by an electric field E.

$$\Delta\left(\frac{1}{n^2}\right)_i = \sum_{j=1}^{3} r_{ij} E_j \quad \ldots (2)$$

where i ranges from 1 and 6, and j corresponds to 1,2, and 3 respectively, associated with the x, y, and z, coordinates. The $6 \times 3\ [r_{ij}]$ matrix, obtained by transforming equation (2) into matrix form, is referred to as the electro-optic tensor. As a result, while building an electro-optic modulator or switch, the waveguide material and its alignment in relation to the applied electric field must be carefully considered. Nonetheless, several low-loss waveguide materials, such as GaAs, GaP, $LiNbO_3$, $LiTaO_3$, and quartz, have extremely high Pockels coefficients for particular orientations. Thus, the linear electro-optic effect is widely used in integrated optics.

Figure 2 shows a planar waveguide constructed utilizing heteroepitaxial growth techniques that may function as a phase modulator, an amplitude modulator, or an optical switch. This waveguide is made of $Ga_{(1-x)}Al_xAs$, however other electro-optic semiconductors such as $GaAs_xP_{(1-x)}$, $GaAs$, or GaP can also be used. Furthermore, reducing carrier concentration is an additional approach to waveguide formation.

2.1 Couple mode theory

The couple mode theory provides a mathematical framework to explain the behaviour of directional couplers and determine their response to external factors[5]. This theory enables precise behavior predictions of the coupler by analyzing the relationship between the channels and the power transfer properties. The validity of the coupled-mode theory in explaining the behavior of the dual-channel directional coupler is confirmed by a comparison between the theoretical model and experimental results[6].

The electric field of the propagating mode in the waveguide for zero applied voltage is expressed as[7].

$$\bar{E}(x,y,z) = A(z).\bar{E}(x,y) \quad \ldots (3)$$

Where A(z) is the complex amplitude which includes the phase term exp(iβz). The term $\bar{E}(x,y)$ is the solution for the field distribution of the mode in one waveguide, assuming that the waveguide is absent. By convention the mode profile $\bar{E}(x,y)$ is assumed to be normalized to carry one unit of power. Thus, the power in core 1 is given by:

$$P_1(z) = |A_1(z)|^2 = A_1(z).A_1^*(z) \quad .. (4)$$

If the modulating signa is applied to the electrodes as shown in Fig. 1, it produces a slight difference in the indices of refraction in the guide, which results in the propagation constant difference Δβ. Following the couple mode theory[5,8].

$$\frac{dA_0(z)}{d_z} = -i.\beta_0.A_0(z) + k_{01}.A_1(z) \quad \ldots (5)$$

$$\frac{dA_1(z)}{d_z} = -i.\beta_1.A_1(z) + k_{10}.A_0(z) \quad \ldots (6)$$

Where β_0 and β_1 are the propagation constant in the two cores, and for the identical guides:

$$k_{01} = k_{10} = -i.k \quad \ldots (7)$$

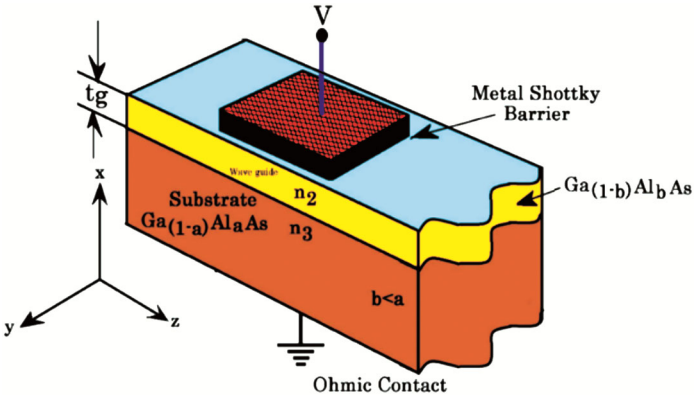

Fig. 2 — Cross-sectional view of Electro-optic modulator as a switch.

Where k is real and k_{01} and k_{10} are the coupling coefficient between the modes. The solution of equations (5) and (6), subject to the boundary condition:

$$A_0(0) = 1 \; and \; A_1(0) = 0 \quad \ldots (8)$$

Yields the following expression for $A_0(Z)$ and $A_1(Z)$.

$$A_0(Z) = \left[\cos(g.z) - i\frac{\Delta\beta}{2g}\sin(g.z)\right].\varepsilon_0 \quad \ldots (9)$$

Where:

$$\varepsilon_0 = exp\left[-i\left(\beta_0 - \frac{\Delta\beta}{2}\right)z\right], and \; A_1(Z) = -\left[\frac{-i.k}{g}.\sin(g.z)\right].\varepsilon_1 \quad \ldots (10)$$

Where:

$$\varepsilon_1 = exp\left[-i\left(\beta_1 + \frac{\Delta\beta}{2}\right)z\right], and \; \Delta\beta = \beta_0 - \beta_1 \ldots (11)$$

$$g^2 \equiv k^2 + \left(\frac{\Delta\beta}{2}\right)^2 \quad \ldots (12)$$

Thus, in the case of imperfect phase match, the power flow in the two cores is expressed as:

$$P_0(z) = A_0(z).A_0^*(z) \quad \ldots (13)$$

$$P_1(z) = A_1(z).A_1^*(z) \quad \ldots (14)$$

The condition for total power transfer for zero applied voltage is expressed as:

$$k.Lc = \frac{\pi}{2} + m.\pi \quad \ldots (15)$$

Where $m = 0,1,2,3,4, \ldots\ldots$, and Lc is the coupling length for the complete power transfer from one core to another. Similarly, equations (13) and (14) results that when modulating voltage is applied to the produce a $\Delta\beta$, the coupling is completely cancelled and can be expressed as $P_1(Lc) = 0 \; and \; P_0(Lc) = 1$ if:

$$g.Lc = \pi + m.\pi \quad \ldots (16)$$

Where $m = 0,1,2,3, \ldots\ldots$

From equations (15) and (16) it can be shown that the value of $\Delta\beta$ required for 100% modulation is given by:

$$(\Delta\beta).Lc = \sqrt{3}\pi \quad \ldots (17)$$

The effective index of refraction in a guide is given by:

$$n_g \equiv \frac{\beta}{k} \quad \ldots (18)$$

Thus, the change in effective index needed for 100% modulation is given by:

$$\Delta n_g = \frac{\sqrt{3}.\pi}{k.Lc} \quad \ldots (19)$$

In typical cases the magnitude of Δn_g required for 100% modulation is surprisingly small. In gallium aluminum arsenide $(GaAlAs) 3\mu m \times 3\mu m$ modulator with directional coupler as shown in Fig. 1, of length 1 cm, and the equation (19) predicts that the light of $900\,nm$ vacuum wavelength can be totally switched from one waveguide to another by producing variation of $\Delta n_g \approx 1 \times 10^{-4}$. From equation (1) the magnitude of required electric field is about $3 \times 10^4 \; V/cm$, corresponding to a voltage of $10 \; Volt$ across $3\mu m$ thick channels[3].

Figure 3 shows that both core 1 and core 2 exhibited identical normalized power strengths when

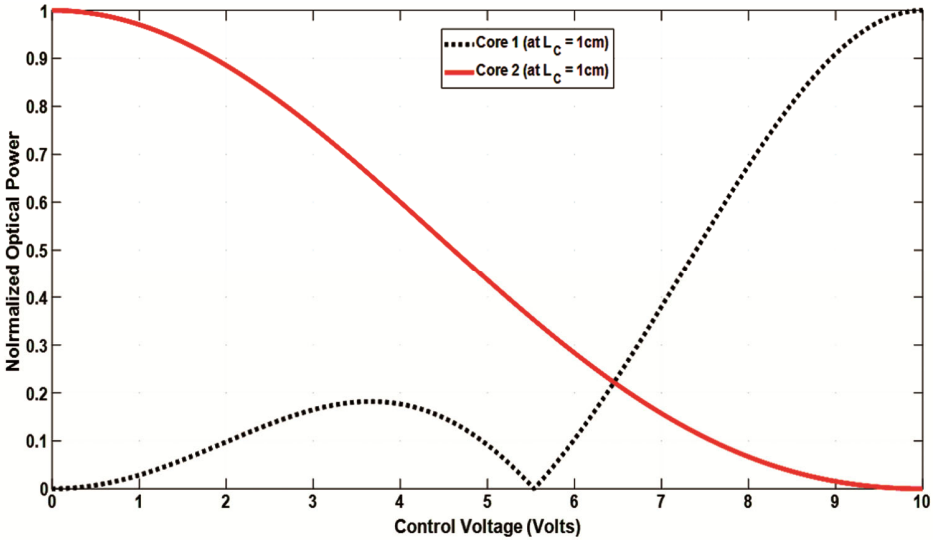

Fig. 3 — Variation of normalized optical power strength at core 1 and core 2 with control voltage V at the coupling length $L_C = 1 \; cm$.

the control voltage was at $V = 0V$. As the control voltage increased, the normalized power in core 2 gradually decreased, while the power in core 1 increased in tandem. This phenomenon can be attributed to the electro-optic effect, wherein the control voltage induces a change in the refractive index of the material, resulting in the redistribution of optical power between the cores. The normalized power strength of core 2 steadily decreased, reaching a minimum value, while the normalized power in core 1 continued to rise, reaching a peak value at the control voltage $V = 10V$ and coupling length $L_C = 1\,cm$. This behavior indicates that increasing the control voltage effectively transfers power from core 2 to core 1. The simulation curve shows the optical switching capability in the EODC when a control voltage is applied.

Figure 4 (a&b) shows the switching activity of an optical pulse in an EODC, which gives vital insights into the operation and characteristics of device. The optical pulse is applied into the input port of EODC, and its path through the device is traced. Variations in the parameters, such as the control voltage, coupling length, or refractive index, of the EODC allow us to see the visual consequences of pulse propagation inside the EODC. Increased control voltage result in power transfer across cores, resulting in power redistribution or total switching of the pulse from one core to another.

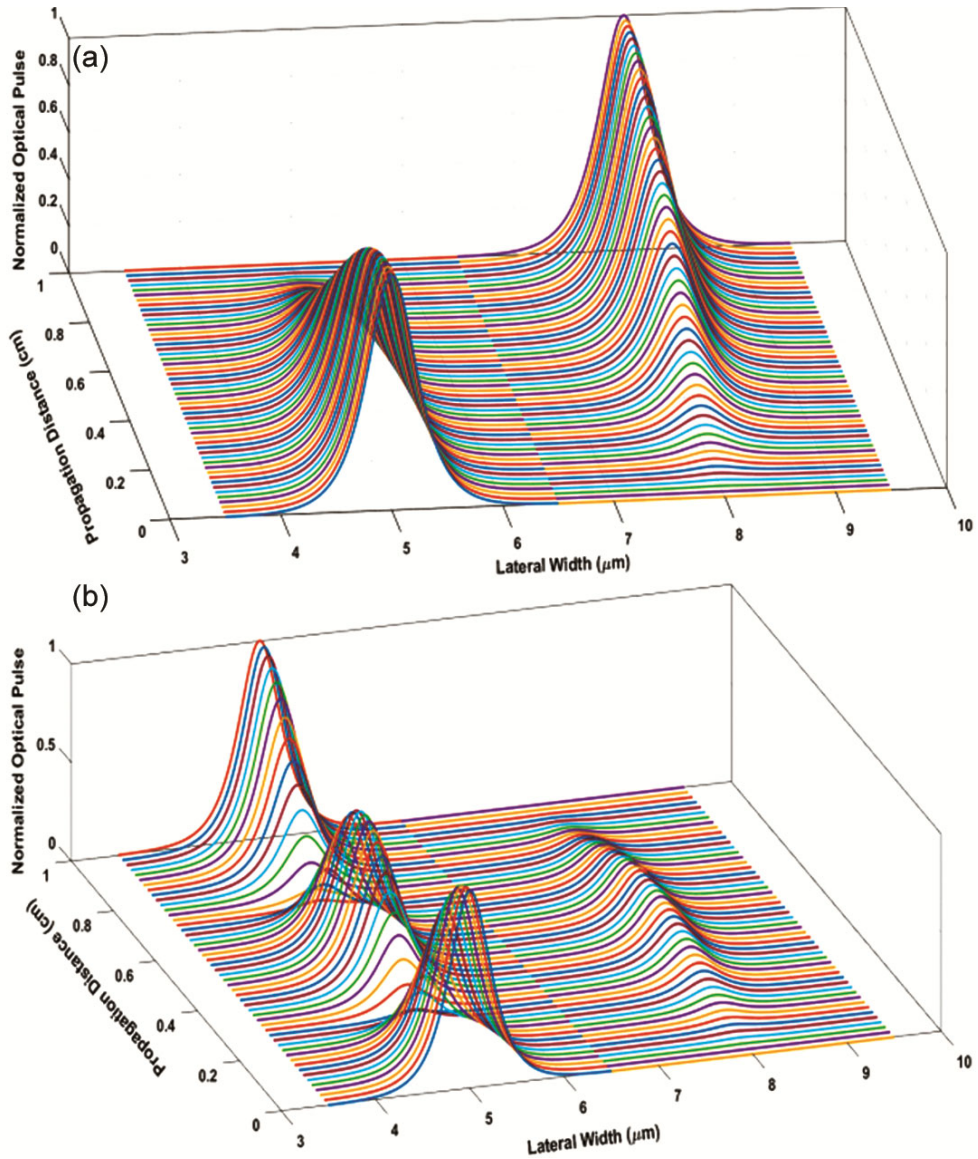

Fig 4 — Switching characteristics of electro-optic effect based optical directional coupler: simulation result of normalized optical pulse propagation along lateral and propagation direction with electrode voltage (a) $V = 0\,V$ (b) $V = 10\,V$.

The presence of an optical pulse indicates an output value of 1, characterized by a high peak of the pulse which corresponds to a control voltage of $10\,V$. Conversely, the absence of a pulse corresponds to an output value of 0 with a pump power of $0\,V$. An optical pulse is applied to the I_1 port of the EODC. After applying a control voltage of $V = 0V$, the signal switches from core 1 to core 2, and emerges with high logic (1) from the O_2 port of the EODC, as shown in Fig. 4(a). When the optical pulse is applied to the I_1 port of the EODC, it propagates along the same waveguide and emerges with high logic (1) at the output port O_1 after applying a control voltage of $V = 10V$, as shown in Fig. 4(b).

3 Implementation of 2:1 MUX using the electro-optic effect-based Directional Couplers

This proposed design explores the significance of 2:1 multiplexer (MUX) in digital circuitry and the role played by optoelectronic components in sophisticated optical communication systems. The simulation approach used for design validation has been utilized to assess the performance of the 2:1 MUX, as shown by the simulation results.

Figure 5 shows the layout design for an optical 2:1 MUX using EODCs. This study presents an introduction to the concept of the 2:1 MUX, emphasizes the importance of electro-optic effects, and provides an explanation of the operational principles behind the optical switching in directional couplers. The proposed design has a high level of detail, and simulation results confirm the propagation of optical pulses inside the proposed 2:1 MUX. The layout design of the proposed device consists of four EODCs, cascaded in a manner to create a 2:1 MUX output. The high optical signal is connected to the O_1 port of DC_1, along with optical energy 2, through the OEM labeled as S_0. The corresponding output of the O_2 port of DC_1 is used as an input to the I_1 port of DC_2, along with optical energy 3. Simultaneously, the output through the O_1 port of DC_1 is fed into the I_2 port of DC_3, along with optical energy 1 (I_1), to activate the E_2 electrode of the EODC. The outputs of DC_2 and DC_3 is then directed as optical energy through the OEM to the E_1 electrode of DC_4. An optical pulse is applied to the I_1 port, and after propagation through the coupler waveguide, the output from the O_1 port corresponds to the 2:1 MUX output, represented as $(\overline{S_0}I_0 + S_0I_0)$.

Figure 6 shows the simulation result of the proposed device which illustrate the optical pulse propagation inside the circuit. Simulation result of the optical 2:1 MUX using the EODC, for the select signal $S_0 = 0\,V$ and Input Signals, (a) $I_1I_0 \rightarrow 00$ which correspond to the low logic output (0), (b) $I_1I_0 \rightarrow 01$which gives the output of high logic 1 , (c) $I_1I_0 = 10$ which gives the output of logic 0, and (d) $I_1I_0 = 11$ which gives the output of logic 1. These results are specifically for the select signal $S_0 = 0\,V$and the corresponding optical input signals to the device: (a) $I_1I_0 \rightarrow 00$, is applied as an optical energy 3 and 1 through OEM, after propagating through the waveguides, the switching phenomenon takes place and the output of the device corresponds to low logic output (0), Similarly, Fig. 6(b) the $I_1I_0 \rightarrow 01$, resulting in a high logic 1 output;

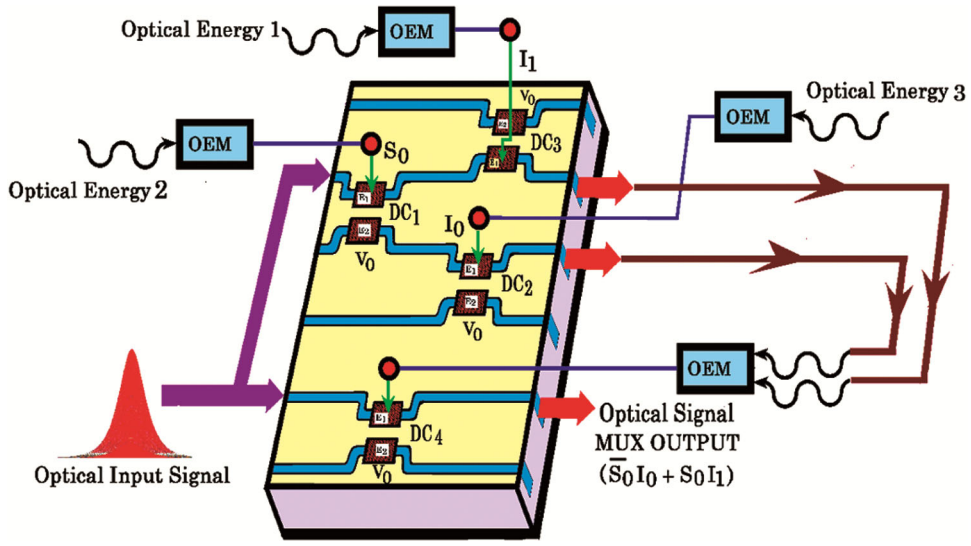

Fig. 5 — Layout design of Optical 2:1 MUX using the electro-optic effect-based switching activity in the Directional Couplers

(c) $I_1 I_0 = 10$, yielding a logic 0 output; and (d) $I_1 I_0 = 11$, producing a logic 1 output for the proposed optical 2:1 MUX using EODC.

Figure 7 shows the output of 2:1 MUX for the logic combination $(00, 01, 10, 11)$ and the select signal $S_0 = 10\ V$. Simulation results confirm the functionality of the 2:1 MUX and visually represent the propagation of optical pulses along the waveguides in the designed circuit. The raised peak of the optical pulse represents a logic high (1), whereas the lower (flat) peak represents

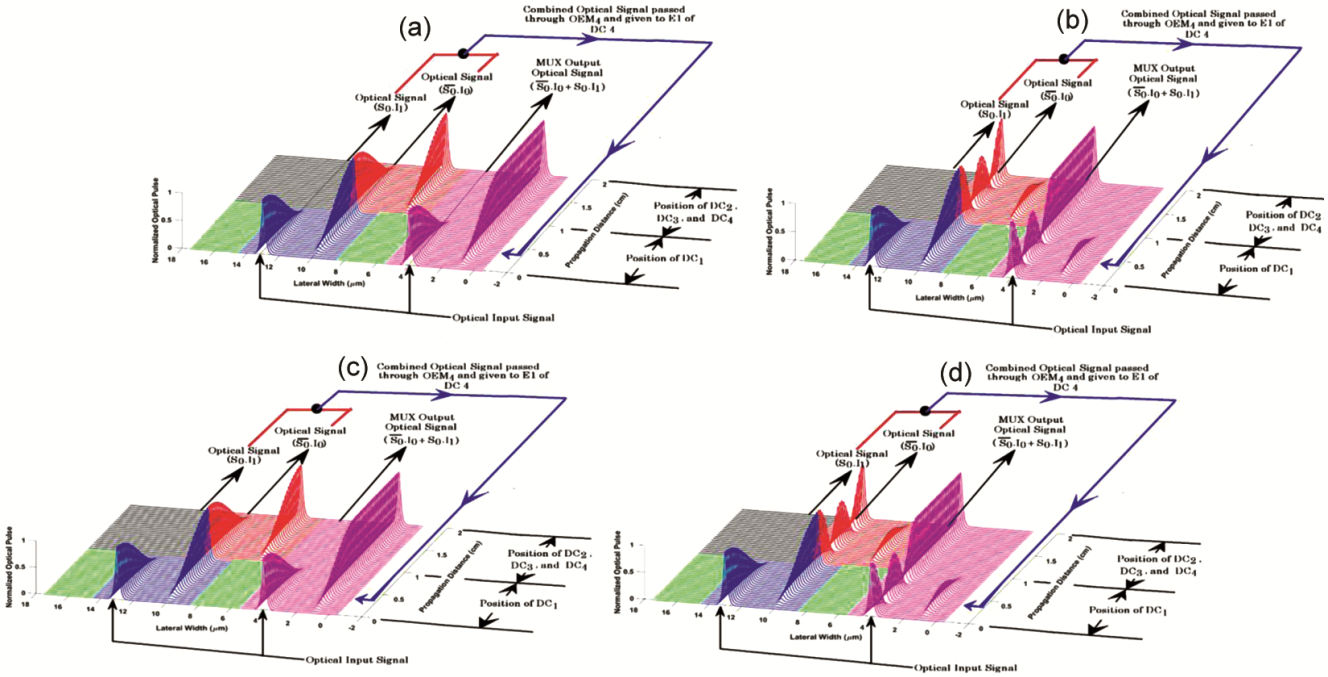

Fig. 6 — Simulation result of the optical 2:1 MUX using the electro-optic effect based directional couplers, for the select signal $S_0 = 0\ V$ and Input Signals, (a) $I_1 = 0\ V\ and\ I_0 = 0\ V$, (b)$I_1 = 0\ V\ and\ I_0 = 10\ V$, (c) $I_1 = 10\ V\ and\ I_0 = 10\ V$, and (d) $I_1 = 10\ V\ and\ I_0 = 10\ V$.

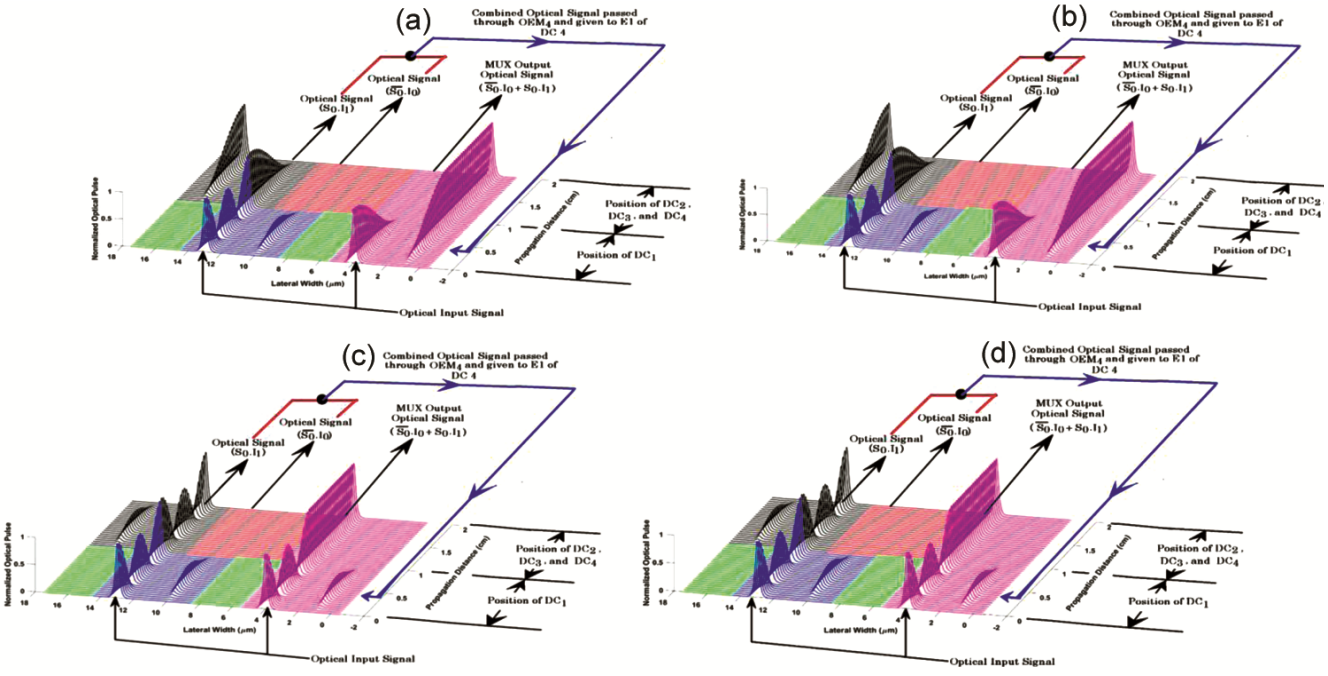

Fig. 7 — Simulation result of the optical 2:1 MUX using the electro-optic effect based directional couplers, for the select signal $S_0 = 10\ V$ and Input Signals, (a) $I_1 = 0\ V\ and\ I_0 = 0\ V$, (b) $I_1 = 0\ V\ and\ I_0 = 10\ V$, (c) $I_1 = 10\ V\ and\ I_0 = 0\ V$, (d) $I_1 = 10\ V\ and\ I_0 = 10\ V$.

a logic low (0). The switching phenomena in DC occur due to the applied voltage across the electrodes of the DC. The existence of an optical pulse implies an output value of 1, with a high peak in the pulse corresponding to a control voltage of 10 V. In contrast, the absence of a pulse results in an output value of 0, with a pump power of 0 V. The functioning of the 2:1 MUX is analyzed under different input logic combinations; it is clear that Fig. 7(a&b) correspond to an output of 0, reflecting specific input conditions ($I_1I_0 = 00\ and\ 01$) such as low voltage. Conversely, Fig. 7(c&d) show a logic 1 output indicating different input scenarios *i.e.*, $I_1I_0 = 10\ and\ 11$.

The design and modeling of an optical 2:1 MUX with EODC demonstrated its efficacy in optical signal routing and data selection, which has been validated through a comparison of the simulation results with established standard results. The use of an optical directional coupler in the design increases the compatibility for RF and microwave applications where signal separation and preservation are essential.

4 Implementation of optical 1:4 DEMUX using electro-optic effect based directional couplers

An optical 1:4 DEMUX (Demultiplexer) is a device that divides a single input optical signal into four output signals ($Y_3, Y_2, Y_1, and\ Y_0$) based on control signals S_1 and S_0. Fig. 8 shows the layout design of the optical 1:4 DEMUX using EODCs is accomplished with the utilization of fourteen optical DCs. Proper cascading is carried out in a manner that ensures the device output corresponds similarly to that of the DEMUX. The OEM serves as a modulator to supply optical energy equivalent to the electrode of the DCs. The optical input signal is applied to the I_1port of DC_1, along with optical energy 1 to the electrode. After propagating through the directional coupler, a switching phenomenon occurs between the cores of DC, and the output ($\bar{S_1}$) is obtained at the O_2 port of DC_1. The $\bar{S_1}$output is then applied as optical energy to DC_{11} and DC_{14}. Similarly, from DC_2, the $\bar{S_0}$ output is obtained and applied as optical energy to DC_8 and DC_{12}.The output Y_3 is obtained through the proper arrangement of $DC_3, DC_4,$ and DC_5, where the optical energy I, S_1, and S_0 is applied to the electrodes, respectively. The output obtained through the O_1 port of DC_5 corresponds to the Y_3 output of the optical 1:4 DEMUX, which is expressed as $(Y_3 = S_1.S_0)$. Similarly, the output Y_2 is obtained from the arrangement of $DC_6, DC_7,$ and DC_8, expressed as $(Y_2 = S_1.\bar{S}_0)$. Y_1 is obtained through $DC_9, DC_{10},$ and DC_{11}, expressed as $(Y_1 = \bar{S_1}.S_0)$, and Y_0 is obtained through $DC_{12}, DC_{13},$ and DC_{14}, expressed as $(Y_0 = \bar{S_1}.\bar{S}_0)$.

Figure 9 shows the Simulation result of the optical $1:4\ DEMUX$ using the EODCs for input signals $(00, 01, 10, 11)$and the select signal $I = 10\ V$. Fig. 9(a) demonstrates the propagation of a pulse within the proposed device. The pulse propagates through the cores of the directional coupler, where the switching of the optical pulse is controlled by supplying voltage to the electrodes of the directional coupler. When the input selects signals $S_1 = 0\ V$ and $S_0 = 0\ V$ are applied to the electrodes as optical energy in conjunction with a high optical

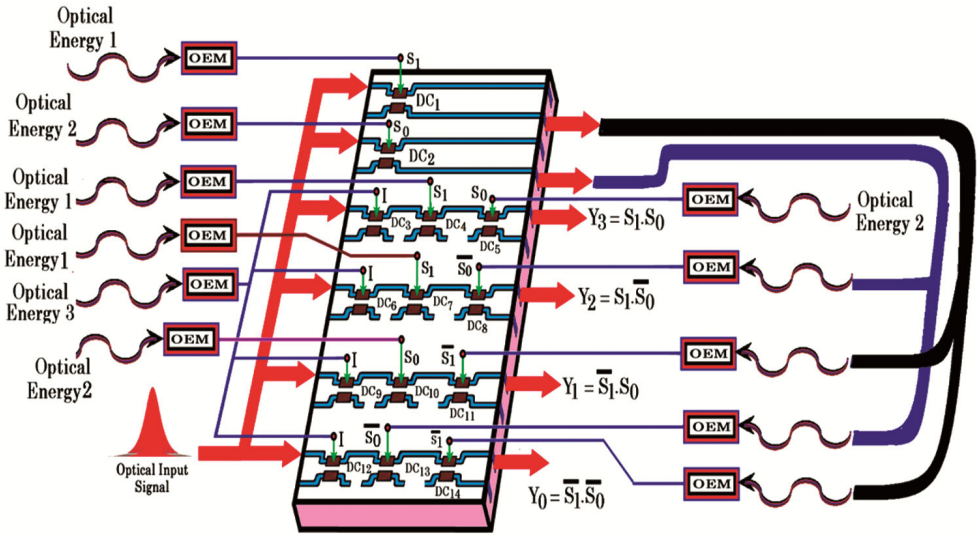

Fig. 8 — Layout design of Optical 1:4 De-multiplexers using the electro-optic effect-based switching activity in the Directional Couplers.

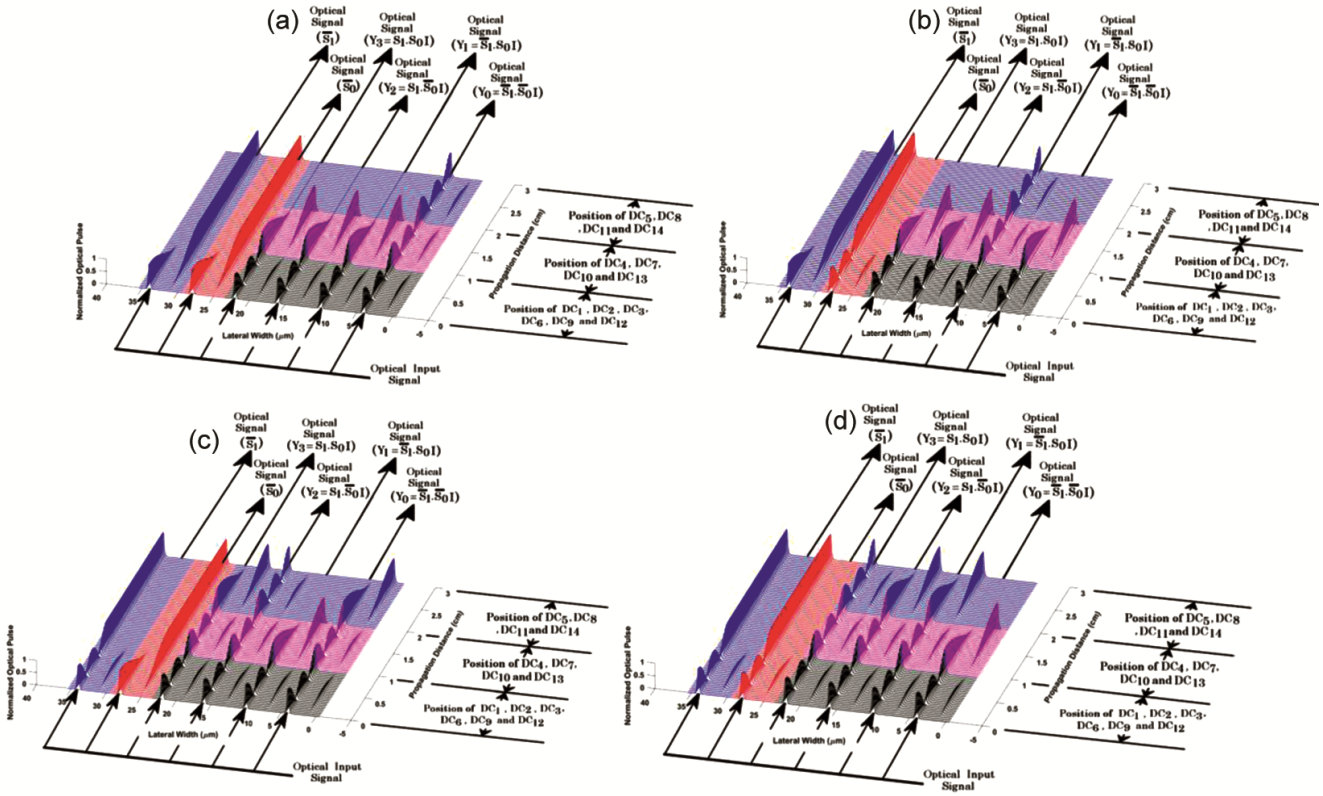

Fig. 9 — Simulation result of the optical $1:4$ $De-multiplexer$ using the electro-optic effect based directional couplers, for input signals, (a) $S_1 = 0\,V, S_0 = 0\,V, I = 10$, (b) $S_1 = 0\,V, S_0 = 10\,V, I = 10\,V$, (c) $S_1 = 10\,V, S_0 = 0\,V, I = 10\,V$, (d) $S_1 = 10\,V, S_0 = 10\,V, I = 10\,V$.

input pulse to the core of the DCs, the resulting output are expressed as $Y_3 = S_1.S_0I$, $Y_2 = S_1.\bar{S}_0I$, $Y_1 = \bar{S}_1.S_0I$, and $Y_0 = \bar{S}_1.\bar{S}_0I$, which results in output values $Y_3Y_2Y_1Y_0 \rightarrow 0001$.Similarly, the output values for the other logic combinations (01, 10, 11) are as follows:$Y_3Y_2Y_1Y_0 \rightarrow 0010, 0100, and\ 1000$,as shown in Figs. 9 (b, c & d) respectively.

The proposed optical 1:4 DEMUX is a critical component that uses control signals to route one optical input to one of four outputs. Its benefits include effective resource utilization, accurate data management, and maintaining signal quality. The device simplifies data routing in applications such as digital communication, memory addressing, and digital displays. It is essential in various electrical and communication systems, improving data distribution efficiency and reducing device costs and size by minimizing the number of components.

5 Implementation of optical 4:2 Encoder Circuit using electro-optic effect based directional couplers

The 4:2 encoder circuit consists of four inputs $(Y_3, Y_2, Y_1, and\ Y_0)$ and two outputs $(A_1 and\ A_0)$. Figure. 10 shows the implementation of a $4:2$ encoder circuit using EODC. The device is designed with six DCs, which allow for the switching of optical pulses within their cores in order to execute the functioning of the proposed optical $4:2$ encoder circuit. An optical input signal is applied to the I_1 port of DC_1, along with the Y_3 control voltage via the OEM. The O_1 output of DC_1 acts as a control voltage for DC_3, while the O_2 output of DC_1 is used as an input signal for DC_2, along with the Y_2 control voltage. Subsequently, an optical input pulse is directed to the I_1 port of DC_3, along with the control voltage (O_1 port output from DC_1 and DC_2), resulting in the A_1 output of the proposed device, which is expressed as $(A_1 = Y_2 + Y_3)$. Similarly, the A_0 output is obtained through the proper configuration of DC_4, DC_5, and DC_6, and it is expressed as $(A_0 = Y_3 + Y_1)$.

Figure 11 shows the simulation results of the proposed optical 4:2 decoder circuit, providing a visual representation of the optical pulse propagation inside the core of DCs. This simulation illustrates the functioning of the decoder circuit and how it operates within the optical domain to generate the desired

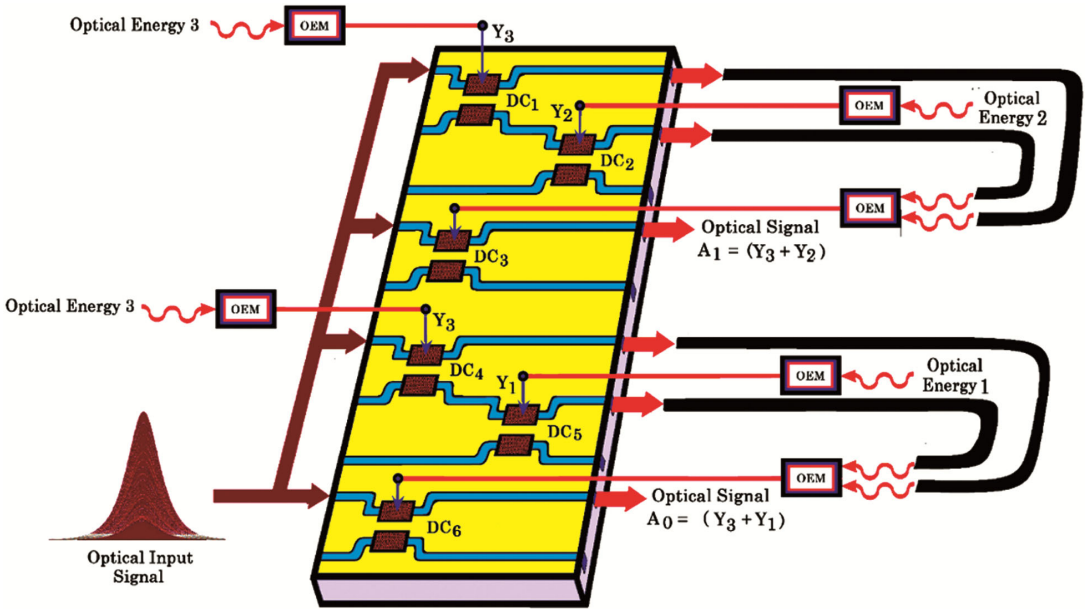

Fig. 10 — Layout design of Optical 4:2 encoder using the electro-optic effect-based switching activity in the Directional Couplers.

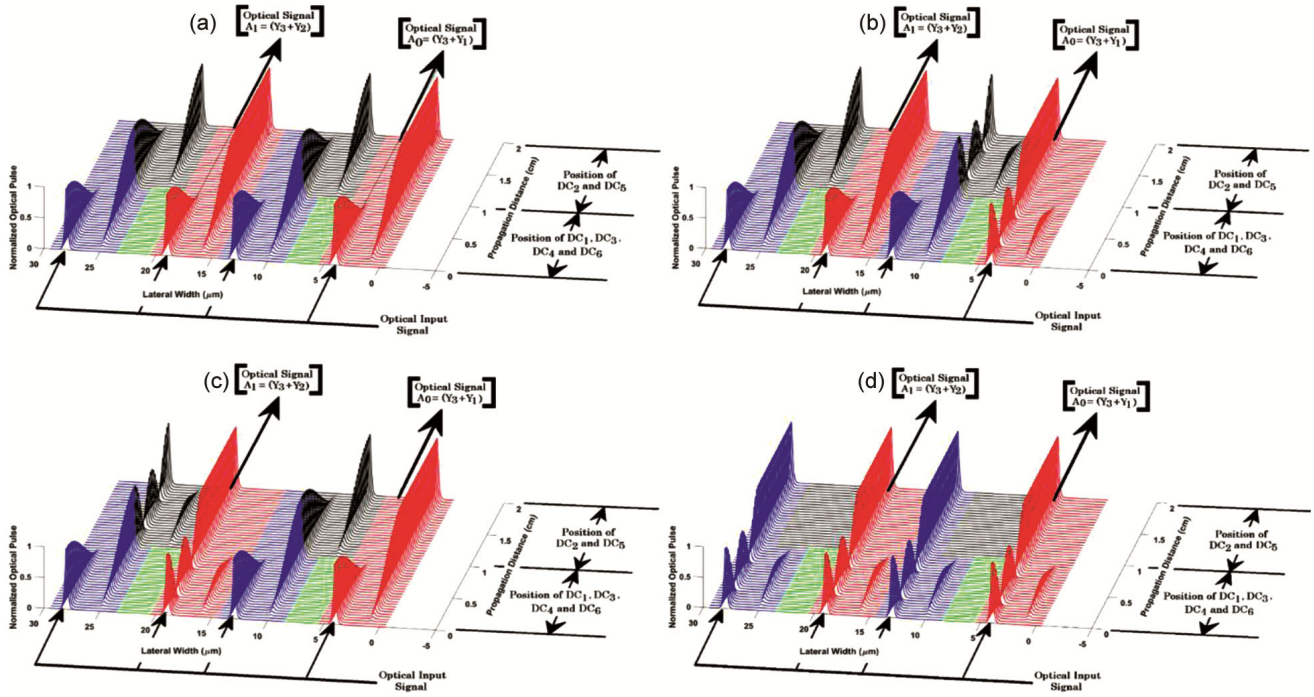

Fig. 11 — Simulation result of the optical 4 : 2 encoder using the electro-optic effect based directional couplers, for input signals, (a) $Y_3 = 0\,V, Y_2 = 0\,V, Y_1 = 0\,V$ *and* $Y_0 = 10\,V$, (b) $Y_3 = 0\,V, Y_2 = 0\,V, Y_1 = 10\,V$ *and* $Y_0 = 0\,V$, (c) $Y_3 = 10\,V, Y_2 = 0\,V, Y_1 = 0\,V$ *and* $Y_0 = 0\,V$, and (d) $Y_3 = 10\,V, Y_2 = 0\,V, Y_1 = 0\,V$ *and* $Y_0 = 0\,V$.

output. The high peak of an optical pulse represents the logic 1 output, while a low optical pulse or a flat pulse represents the logic 0 output. Fig. 11(a) shows the simulation results for the input logic combination $Y_3Y_2Y_1Y_0 \rightarrow 0001$, which corresponds to the outputs $A_1 = 0$ and $A_0 = 0$, expressed as $A_1 = Y_3 + Y_2$ and $A_0 = Y_3 + Y_1$. $A_1 = 0$. Similarly, Fig. 11 (b,c&d) show the simulation results for the remaining input logic combinations, *i.e.*, $Y_3Y_2Y_1Y_0 \rightarrow 0010$, 0100 and 1000, which correspond to the outputs $A_1A_0 \rightarrow 01$, $A_1A_0 \rightarrow 10$, and $A_1A_0 \rightarrow 11$, respectively.

Optical encoders are essential in optical communication systems, where they transform electrical signals into light pulses for transmission via optical fibers, as well as in optical storage media, such as CDs and DVDs, where they encode and decode data. Essentially, optical encoders operate with light-based signals to enable effective data processing and transfer in optical communication systems. The simulation results are compared with standard results to verify the accuracy of the circuit.

6 Implementation of optical 2:4 Decoder circuit using the electro-optic effect-based directional couplers

Implementation of an optical 2:4 Decoder circuit employing EODC significantly contributes to the burgeoning field of optics. This work delves into the intricate dynamics of light manipulation, electric field modulation, and signal processing within the realm of optical communication and computation. The findings of this study demonstrate substantial potential for advancing and utilizing cutting-edge information processing technologies across diverse real-world applications.

Figure 12 shows the elaborate design and implementation of the proposed circuit using EODCs on a single substrate. The device is delicately constructed of ten meticulously organized DCs that are strategically cascaded to produce the precise functioning of a 2:4 decoder. Initially, the input directional couplers (DC_1 and DC_2) are applied with an input optical signal, and the A_1 and A_0 inputs to the electrodes of the EODCs, directing them towards subsequent stages. The output of the directional couplers relies on the input optical energy to the electrode of DC_1, which is then routed to the electrodes of DC_3 and DC_6. Similarly, for DC_2, the output is directed to the electrodes of DC_4 and DC_8. Additionally, the OEM channels the optical energies A_0 and A_1 to the electrodes of the EODCs, facilitating efficient signal modulation within the system. The cascaded DCs, including DC_4, DC_6, DC_8, and DC_{10}, collaborate to produce the 2:4 decoder outputs. DC_4 generates the output $Y_0(Y_0 = \overline{A_1}.\overline{A_0})$, DC_6 generates the output $Y_1(Y_1 = \overline{A_1}.A_0)$, DC_8 generates the output $Y_2(Y_2 = A_1.\overline{A_0})$, and DC_{10} generates the output $Y_3(Y_3 = A_1.A_0)$, effectively decoding the input optical signals into the desired decoder output.

Figure 13 shows the complete simulation of the propagation of optical pulses within the core of the DCs. Coupled wave theory accurately describes the interaction between the optical signal and the coupler structure, shedding light on the complex coupling dynamics and energy transfer processes from one core

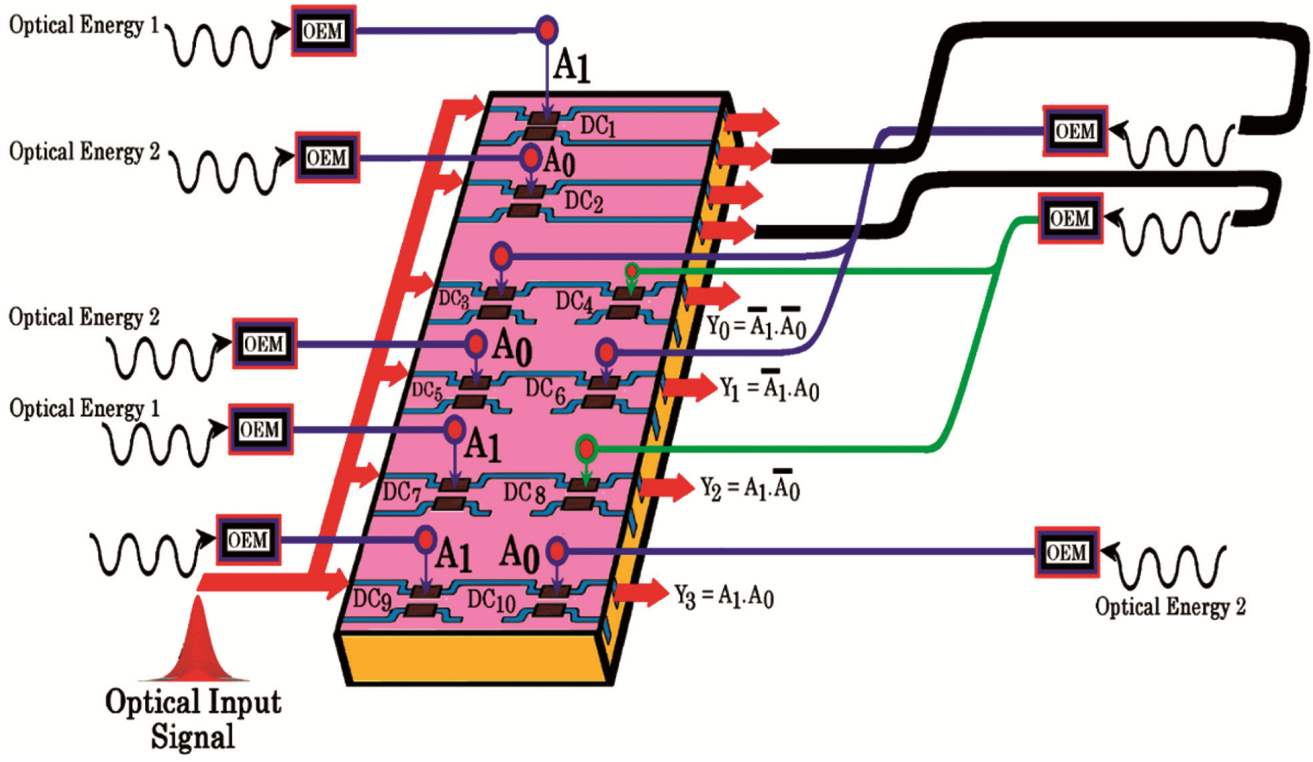

Fig. 12 — Layout design of Optical 2:4 Decoder using the electro-optic effect-based switching activity in the Directional Couplers

to the other. Insight into pulse development is gained by examining factors such as refractive index profile and coupler length and analyzing the effect of these elements on signal quality and transmission efficiency. The simulation findings provide a deeper understanding of pulse behavior, emphasizing directional coupler design feasibility and use for high-fidelity optical signal processing and advanced circuit design. Fig. 13(a) shows the simulation result for the optical input combinations $A_1 = 0\,V\ and\ A_0 = 0\,V$, yielding $Y_3Y_2Y_1Y_0 \rightarrow 0001$. Similarly, Fig. 13(b) displays the simulation result for the optical input combinations $A_1 = 0\,V\ and\ A_0 = 10\,V$, resulting in $Y_3Y_2Y_1Y_0 \rightarrow 0010$. In addition, Fig. 13(c) exhibits the simulation result for the optical input combinations $A_1 = 10\,V\ and\ A_0 = 0\,V$, producing $Y_3Y_2Y_1Y_0 \rightarrow 0100$. Lastly, Fig. 13(d) showcases the simulation result for the optical input combinations $A_1 = 10\,V\ and\ A_0 = 10\,V$, yielding $Y_3Y_2Y_1Y_0 \rightarrow 1000$.

The design of an optical 2:4 decoder circuit based on the electro-optic effect using directional couplers. Simulation results validate the correctness of the design, demonstrating alignment with the standard results of the proposed device.

7 Implementation of Optical Priority Encoder Circuits using the Electro-optic Effect-based Directional Couplers

The encoder prioritizes incoming signals and outputs a binary code that reflects the highest priority input. Fig. 14 shows the layout design implementation of Optical 4:2 Priority Encoder ($I_3 \rightarrow I_0$ as highest priority) using the nine EODCs. The electrode inputs control signals ($I_3, I_2, I_1,$ and I_0) in the EODCs suggest the utilization of the electro-optic effect, where the applied voltage modifies the refractive index of the waveguides. By altering the refractive index, the coupling behaviour of the waveguides can be changed, thereby enabling control and switching of the optical signals. The input optical signal is applied to the electrode of DC_1 along with the input control signalI_3, serving as a control voltage to the electrode. The output from the O_2 port is then used as an input signal to DC_2, along with the I_2 input to the electrode. The outputs from DC_1 and DC_2 are applied as control voltages to DC_3, along with the optical signal at the input port. This process results in the production of the output Y_1 of the encoder circuit, expressed as $(Y_1 = I_3 + I_2)$.Similarly, the Y_0output is obtained by

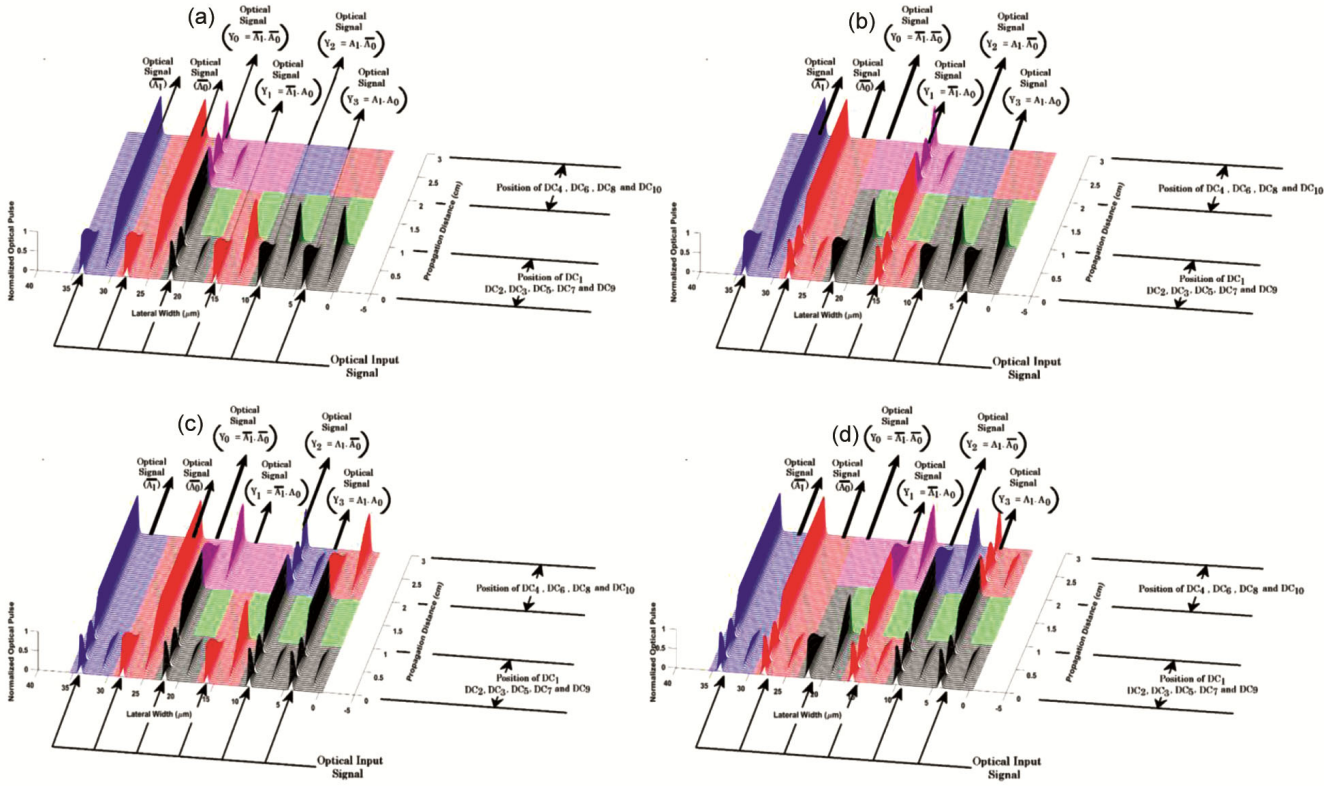

Fig. 13 — Simulation result of the optical 2 :4 Decoder using the electro-optic effect based directional couplers, for input signals, (a) $A_1 = 0\,V\ and\ A_0 = 0\,V$, (b) $A_1 = 0\,V\ and\ A_0 = 10\,V$, (c) $A_1 = 10\,V\ and\ A_0 = 0\,V$, and (d) $A_1 = 10\,V\ and\ A_0 = 10\,V$.

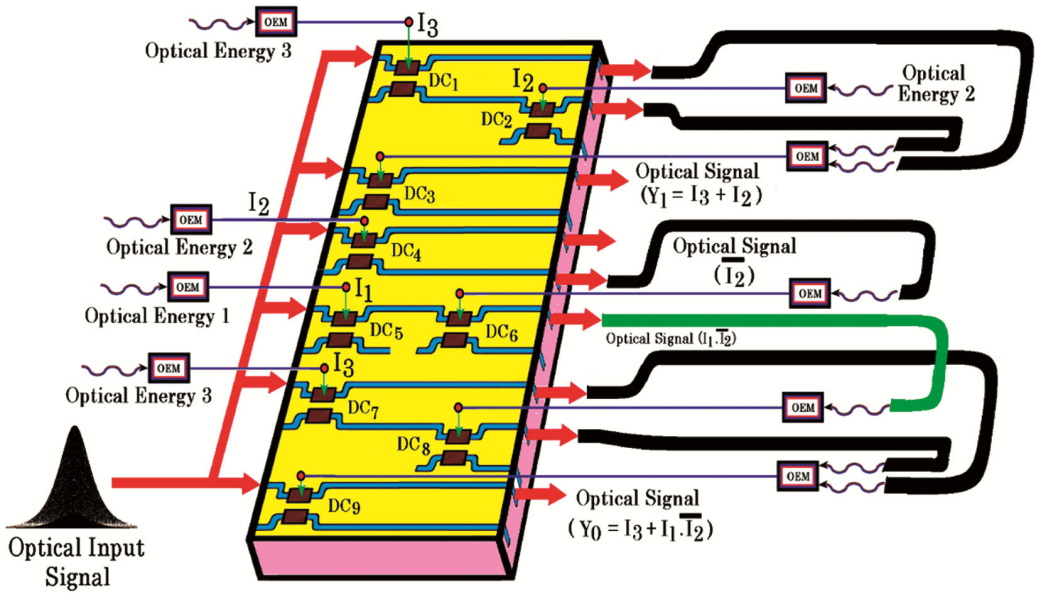

Fig. 14 — Layout design of Optical 4:2 Priority Encoder ($I_3 \rightarrow I_0$ as highest priority) using the electro-optic effect-based switching activity in the Directional Couplers

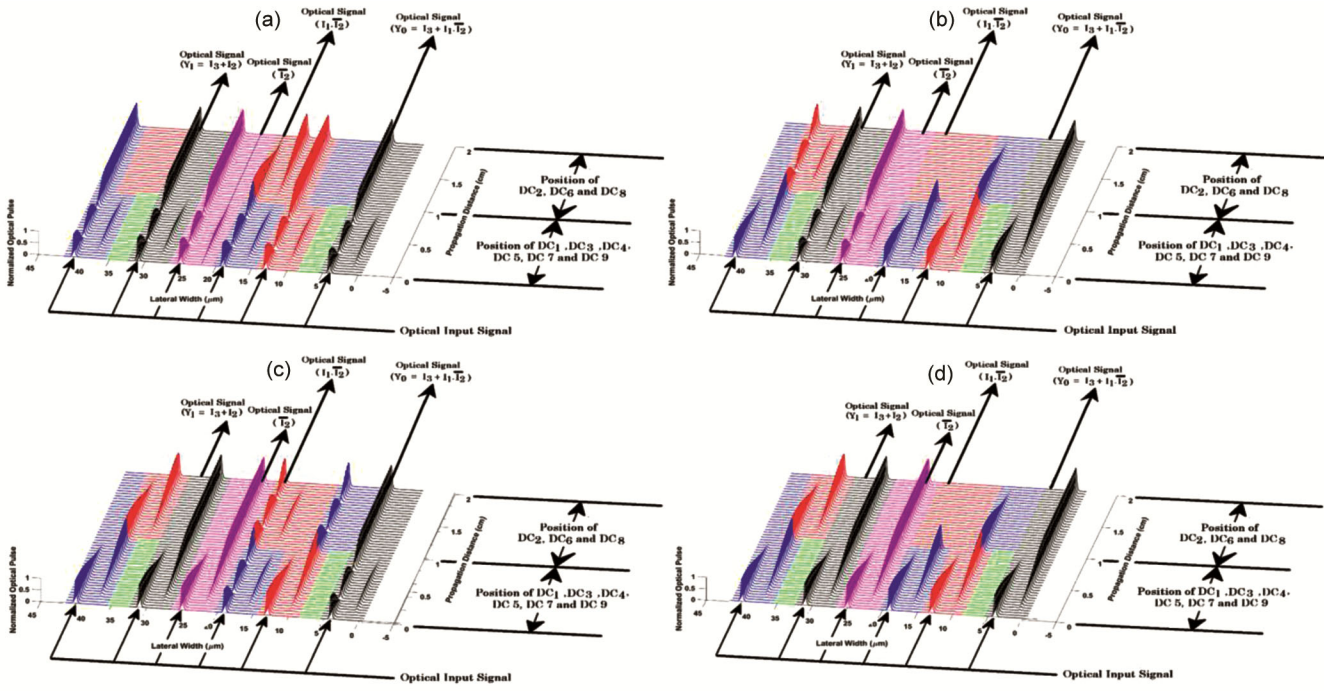

Fig. 15 — Simulation result of the optical 4:2 Priority Encoder using the electro-optic effect based directional couplers, for input signals, (a) $I_3 = 10\,V, I_2 = 10\,V, I_1 = 10\,V$ *and* $I_0 = 0\,V$, (b) $I_3 = 0\,V, I_2 = 10\,V, I_1 = 0\,V$ *and* $I_0 = 0\,V$, (c) $I_3 = 0\,V, I_2 = 0\,V, I_1 = 10\,V$ *and* $I_0 = 0\,V$, (d) $I_3 = 0\,V, I_2 = 0\,V, I_1 = 0\,V$ *and* $I_0 = 10\,V$.

appropriately cascading directional couplers $DC_3, DC_4, DC_5, DC_6, DC_7, DC_8$, and DC_9 with the relevant input control voltages I_3, I_2, and I_1. The internal switching occurs within the cores of these directional couplers, and the output of DC_9 yields the Y_0 output of the optical 4:2 priority encoder ($I_3 \rightarrow I_0$ having the highest priority), expressed as ($Y_0 = I_3 + I_1.\overline{I_2}$).

The simulation findings are critical for comprehending the operation of device as well as its prospective uses in optical communication technology. Fig. 15 shows the simulation results of

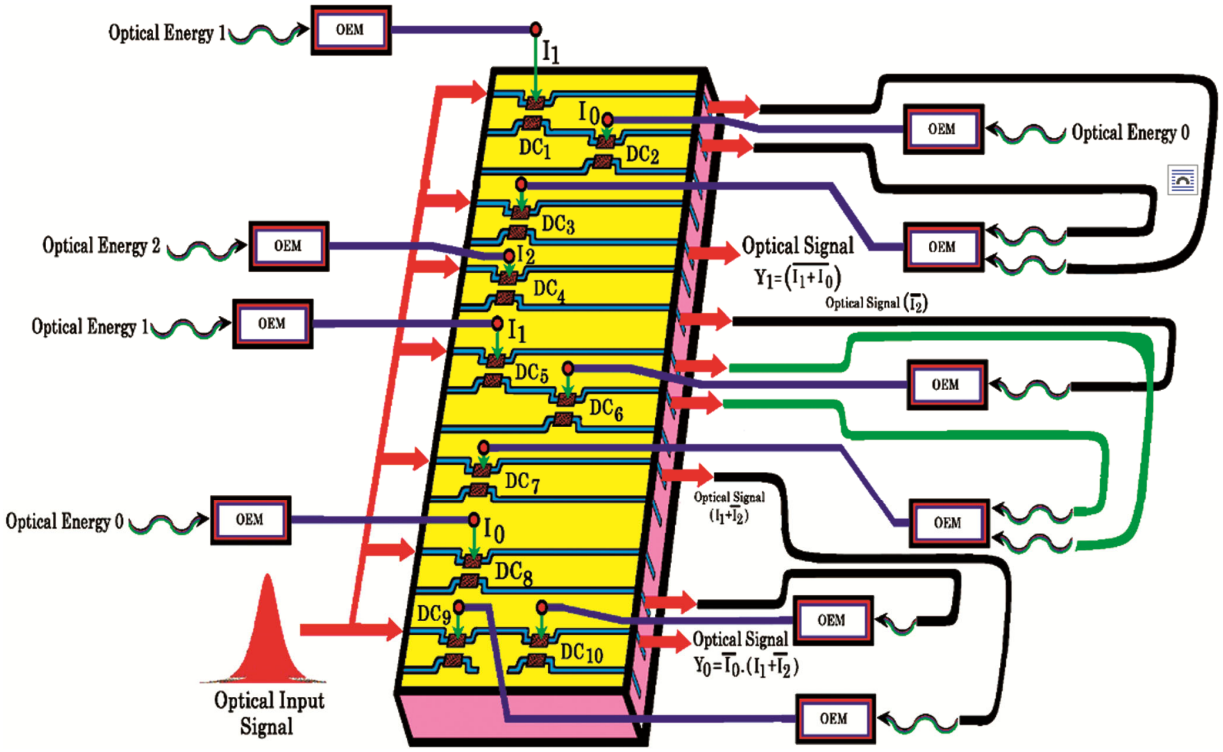

Fig. 16 — Layout design of Optical 4:2 Priority Encoder ($I_0 \rightarrow I_3$ as highest priority) using the electro-optic effect-based switching activity in the Directional Couplers

the proposed device for the input control signals $(I_3, I_2, I_1, and\ I_0)$, exhibiting the pulse propagation inside the cores of the directional coupler. The higher peak of the optical pulse at the output port of the DCs represents the high logic (1), while the flat pulse indicates the low logic (0). Fig. 15(a), the switching mechanism of the proposed device for the input combination $I_3 = 10\,V, I_2 = 10\,V, I_1 = 10\,V, and\ I_0 = 0\,V$ corresponds to the output $Y_1 = 1\ and\ Y_0 = 1$. Similarly, Fig. 15(b) demonstrates the switching mechanism of the encoder circuit for the input combination $I_3I_2I_1I_0 \rightarrow 0100$, resulting in $Y_1 = 1$ and $Y_0 = 0$, Fig. 15(c) illustrates the switching mechanism of the encoder circuit for the input combination $I_3I_2I_1I_0 \rightarrow 0010$, resulting in $Y_1 = 0$ and $Y_0 = 1$, and Fig. 15(d) displays the switching mechanism of the encoder circuit for the input combination $I_3I_2I_1I_0 \rightarrow 0001$, resulting in $Y_1 = 0$ and $Y_0 = 0$.

Figure 16 shows the layout implementation of an optical 4:2 priority encoder circuit, with $I_0 \rightarrow I_3$ as highest priority. The circuit operates using an optical input signal and input control voltages $(I_3, I_2, I_1, and\ I_0)$, with ten EODCs arranged in a specific configuration to achieve the desired operation. Now, the control voltage I_1 is applied to the electrode of DC_1, while the optical input signal serves as an input to the O_1 port of DC_1. The output of DC_1 is then used as an input to DC_2, alongside control voltage I_0. The outputs of DC_1 and DC_2 function as control voltages for DC_3, in conjunction with the optical input signal at the input port. The resulting output from DC_3 represents the optical output (Y_1) of the device, which can be mathematically expressed as $(Y_1 = \overline{I_1 + I_0})$. Similarly, the output Y_0 is obtained using the proper switching mechanism inside $DC_4 \rightarrow DC_{10}$. The optical output Y_0 is obtained from the O_1 port of DC_{10}, expressed as $\left(Y_0 = \overline{I_0}.(I_1 + \overline{I_2})\right)$.

Figure 17 shows the simulation results of the designed optical 4:2 priority encoder circuit (with $I_0 \rightarrow I_3$ as the highest priority) using EODCs. The simulation process follows the same procedure as the earlier simulation of the optical priority encoder (with $I_3 \rightarrow I_0$ as the highest priority).The simulation illustrates the propagation of pulses within the core of the directional couplers, demonstrating the switching mechanism and presenting the results for the proposed device. Fig. 17(a), the switching mechanism of the proposed device for the input combination $I_3 = 10\,V, I_2 = 0\,V, I_1 = 0\,V, and\ I_0 = 10\,V$ corresponds

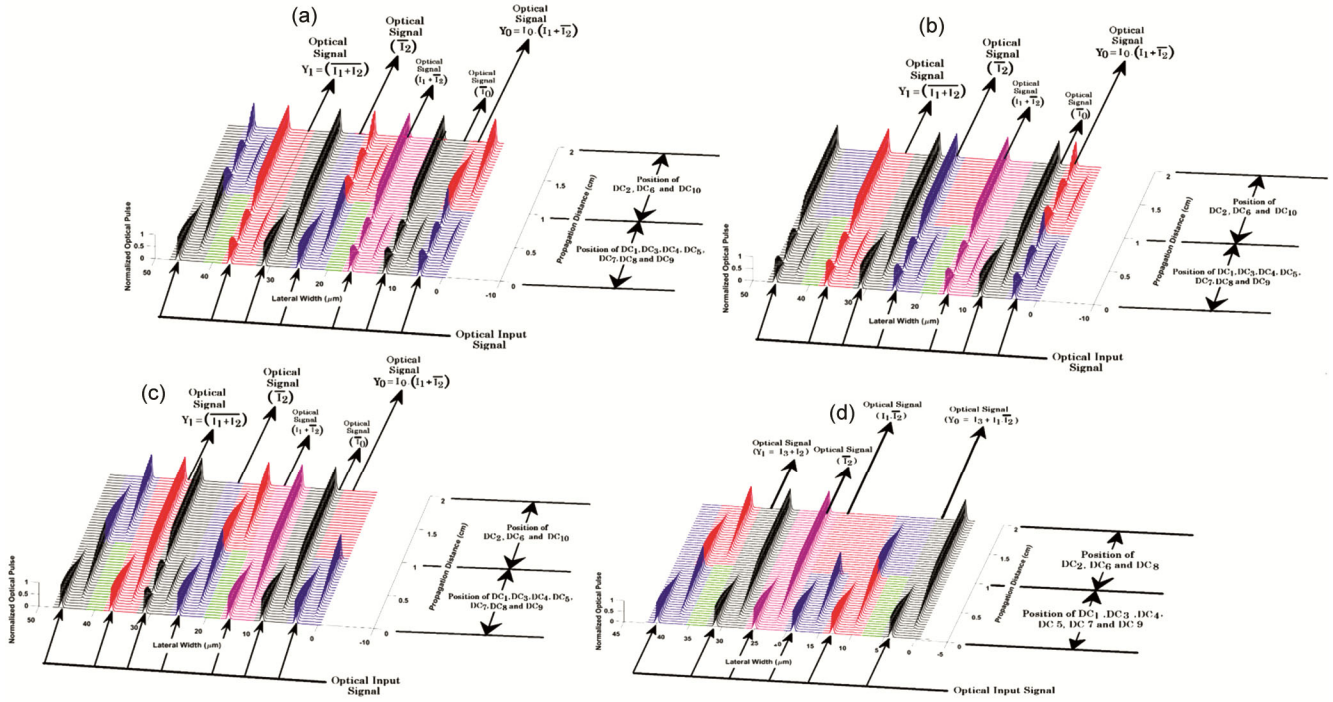

Fig. 17 — Simulation result of the optical 4:2 Priority Encoder using the electro-optic effect based directional couplers, for input signals, (a) $I_3 = 10\,V, I_2 = 0\,V, I_1 = 0\,V$ *and* $I_0 = 10\,V$, (b) $I_3 = 10\,V, I_2 = 0\,V, I_1 = 10\,V$ *and* $I_0 = 0\,V$, (c) $I_3 = 10\,V, I_2 = 10\,V, I_1 = 0\,V$ *and* $I_0 = 0\,V$, (d) $I_3 = 10\,V, I_2 = 0\,V, I_1 = 0\,V$ *and* $I_0 = 0\,V$.

to the output $Y_1 = 0$ and $Y_0 = 0$. Similarly, Fig. 17(b) demonstrates the switching mechanism of the encoder circuit for the input combination $I_3I_2I_1I_0 \rightarrow 1010$, resulting in $Y_1 = 0$ and $Y_0 = 1$, Fig. 17(c) illustrates the switching mechanism of the encoder circuit for the input combination $I_3I_2I_1I_0 \rightarrow 1100$, resulting in $Y_1 = 1$ and $Y_0 = 0$, and 17 (d) displays the switching mechanism of the encoder circuit for the input combination $I_3I_2I_1I_0 \rightarrow 1000$, resulting in $Y_1 = 1$ and $Y_0 = 1$.

8 Conclusion

The work demonstrates that using the electro-optic effect in a directional coupler circuit can design and execute optical digital data transmission circuits. The encoder, decoder, priority encoder, integrated MUX, and DEMUX circuits work together to create a reliable and effective data transmission system. To implement the design aspect of the proposed circuits basic switching mechanism is shown which represents the NOT gate functionality. The proposed device layout is made of $GaAlAs$ material and has a modulator with dimension of $3\mu m \times 3\mu m$. The coupling length (L_C) of the device is set to $L_C = 1\,cm$. The EODC performs perfect switching with a light wavelength of $900\,nm$ by creating a refractive index change (Δn) of approximately $\Delta n \cong 1 \times 10^{-4}$. An electric field magnitude of approximately $3 \times 10^4 V/cm$ is required to achieve this switching, which corresponds to a voltage of 10 V applied across the electrodes of an EODC over a $3\mu m$ channel.The presence of an optical pulse corresponds to an output value of 1, indicated by a high pulse peak aligned with a control voltage of 10 V. Conversely, the absence of a pulse indicates an output value of 0, accompanied by a pump power of 0 V. Simulation results illustrate that the suggested optical devices offer fast signal processing and low energy consumption, representing significant progress in optical communications technology. This research demonstrates the feasibility of advanced photonic circuit design, presenting new possibilities for data transmission and error-detection systems through the integration of directional couplers based on the electro-optic effect.

References

1 Agrawal G P, *Fiber-Optic Communication Systems*, Wiley, (2010).
2 Degeratu V, Schiopu P & Degeratu S, *2001 Int Semiconduct Conf CAS,* (2001) 209.
3 Degeratu V, Schiopu P & Degeratu S, *Int Semiconduct Conf CAS*, (2001) 213.

4 Yariv A, *Quantum Electronics*. John Wiley & Sons, (1989).
5 Yariv A, *Introduction to Optical Electronics*, 2nd Edn, Holt, Rinehart and Winston, 9780030898921 (1976).
6 Peall R G & Syms R R A, *IEEE J Quantum Electron*, 25 (1989) 729.
7 Hunsperger R G, *Integrated optics: Theory and technology:* 6th Edn, Springer US, (2009).
8 Haus H A, *Waves and fields in optoelectronics*, Prentice-Hall, Englewood Cliffs, N J, (1984).
9 Singh L, Saxena R, Zho G, Saha C & Pareek P, *Opt Commun*, 522 (2022) 128707.
10 Tripathy S K, Sahu S, Mohapatro C & Dash S P, *Opt Commun*, 285 (2012) 3234.
11 Charles I, Swarnakar S, Nalubolu G R, Palacharla V & Kumar S, *Photonics*, 10 (2023) 74.
12 Nanda R, Rath R, Swarnakar S & S Kumar, *Plasmonics*, 17 (2022) 2153.
13 Ding Y, Xu J, Ros F Da, Huang B, Ou H & Peucheret C, *Opt Express*, 21 (2013) 10376.
14 Nitiss E, *J Nanophoton*, 11 (2017) 016013.
15 Yang S-Y, Chung H-P, Yang S-L, Chien T-Y, Huang K-H & Chen Y-H, *Opt Commun*, 458 (2020) 124800.
16 Jindal P, Houran M A, Goyal D & Choudhary A, *Optik (Stuttg)*, 280 (2023) 170794.
17 Huang Y, Shi M, Yu A & Xia L, *Appl Opt*, 62 (2023) 774.
18 Yadav A, Kumar A & Prakash A, *Optik (Stuttg)*, 288 (2023) 171190.
19 Liang H, Soref R, Mu J, Li X & Huang W-P, *Appl Opt*, 54 (2015) 5897.
20 Awasthi S, *et al.*, *Appl Opt*, 60 (2021) 4544.
21 Kumar S, Bisht A, Singh G & Amphawan A, *Opt Quantum Electron*, 47 (2015) 3667.
22 Kumar S, Singh G & Bisht A, *Opt Commun*, 353 (2015) 17.
23 Kumar S, Singh L & Chen N-K, *Plasmonics*, 13 (2018) 1277.
24 Anagha E G & Jeyachitra R K, *Opt Eng*, 61 (2022).
25 Stegeman G I & Wright E M, *All-optical waveguide switching*, (1990).
26 Chakraborty R, Biswas J C & Lahiri S K, *Opt Commun*, 219 (2003) 157.
27 Jiu-Sheng L, Han L & Le Z, *Opt Commun*, 350 (2015) 248.
28 Shalaby H M H, *J Lightwave Technol*, 34 (2016) 3633.
29 Ni B & Xiao J, *Opt Commun*, 451 (2019) 141.
30 Chen J, *Optik (Stuttg)*, 202 (2020) 163602.